# A frontal projection-type three-dimensional display

**Youngmin Kim,[1,2] Keehoon Hong,[1] Jiwoon Yeom,[1] Jisoo Hong,[1] Jae-Hyun Jung,[1] Yong Wook Lee,[3] Jae-Hyeung Park,[4] and Byoungho Lee[1,*]**

[1]*School of Electrical Engineering, Seoul National University, Gwanak-Gu Gwanakro 1, Seoul 151-744, South Korea*
[2]*Realistic Media Platform Research Center, Korea Electronics Technology Institute, Mapo-Gu Sangam-Dong, Seoul 121-835, South Korea*
[3]*School of Electrical Engineering, Pukyong National University, Nam-Gu Daeyeon 3-Dong, Busan 608-737, South Korea*
[4]*School of Electrical & Computer Engineering, Chungbuk National University, Heungduk-Gu Cheongju-Si, Chungbuk 361-763, South Korea*
[*]*byoungho@snu.ac.kr*

**Abstract:** In a typical auto-stereoscopic three-dimensional display, the parallax barrier or lenticular lens is located in front of the display device. However, in a projection-type auto-stereoscopic display, such optical components make it difficult to display elemental images on the screen or to reconstruct a three-dimensional image, even though a projection-type display has many advantages. Therefore, it is necessary to use a rear projection technique in a projection-type auto-stereoscopic display, despite the fact that this is an inefficient use of space. We propose here a frontal projection-type auto-stereoscopic display by using a polarizer and a quarter-wave retarding film. Since the proposed method uses a frontal projection scheme and passive polarizing components, it has the advantage of being both space saving and cost effective. This is the first report that describes a frontal projection-type auto-stereoscopic display based on a parallax barrier and integral imaging by using a projector. Experimental results that support the proposed method are provided.



**OCIS codes:** (110.2990) Image formation theory; (100.6890) Three-dimensional image processing; (220.2740) Geometric optical design.

## References and links

1. B.-W. Lee, I.-H. Ji, S. M. Han, S.-D. Sung, K.-S. Shin, J.-D. Lee, B. H. Kim, B. H. Berkeley, and S. S. Kim, "Novel simultaneous emission driving scheme for crosstalk-free 3D AMOLED TV," SID Int. Symp. Digest Tech. Papers **41**, 758–761 (2010).
2. H. Kang, S.-D. Roh, I.-S. Baik, H.-J. Jung, W.-N. Jeong, J.-K. Shin, and I.-J. Chung, "A novel polarizer glasses-type 3D displays with a patterned retarder," SID Int. Symp. Digest Tech. Papers **41**, 1–4 (2010).
3. S. B. Steinman, B. A. Steinman, and R. P. Garzia, *Foundations of Binocular Vision: A Clinical Perspective* (McGraw-Hill, 2000), Chap. 7.
4. H. Liao, M. Iwahara, N. Hata, and T. Dohi, "High-quality integral videography using a multiprojector," Opt. Express **12**(6), 1067–1076 (2004).
5. J. Kim, Y. Kim, H. Choi, S.-W. Cho, Y. Kim, J. Park, G. Park, S.-W. Min, and B. Lee, "Implementation of polarization-multiplexed tiled projection integral imaging system," J. Soc. Inf. Disp. **17**(5), 411–418 (2009).
6. J. Arai, M. Okui, T. Yamashita, and F. Okano, "Integral three-dimensional television using a 2000-scanning-line video system," Appl. Opt. **45**(8), 1704–1712 (2006).
7. Y. Kim, S. G. Park, S.-W. Min, and B. Lee, "Projection-type integral imaging system using multiple elemental image layers," Appl. Opt. **50**(7), B18–B24 (2011).
8. D.-Q. Pham, N. Kim, K.-C. Kwon, J.-H. Jung, K. Hong, B. Lee, and J.-H. Park, "Depth enhancement of integral imaging by using polymer-dispersed liquid-crystal films and a dual-depth configuration," Opt. Lett. **35**(18), 3135–3137 (2010).
9. Y. Jeong, S. Jung, J.-H. Park, and B. Lee, "Reflection-type integral imaging scheme for displaying three-dimensional images," Opt. Lett. **27**(9), 704–706 (2002).
10. J.-S. Jang and B. Javidi, "Three-dimensional projection integral imaging using micro-convex-mirror arrays," Opt. Express **12**(6), 1077–1083 (2004).

#168826 - $15.00 USD Received 17 May 2012; revised 24 Jun 2012; accepted 17 Jul 2012; published 20 Aug 2012

11. Y. Kim, S. G. Park, S.-W. Min, and B. Lee, "Integral imaging system using a dual-mode technique," Appl. Opt. **48**(34), H71–H76 (2009).
12. J. Hong, Y. Kim, S. G. Park, J.-H. Hong, S.-W. Min, S.-D. Lee, and B. Lee, "3D/2D convertible projection-type integral imaging using concave half mirror array," Opt. Express **18**(20), 20628–20637 (2010).
13. W. Jang, Y. W. Lee, J. Oh, and Y. W. Lee, "Inline conversion between transmission and reflection spectra of fiber Bragg grating using polarization-diversity loop structure," IEEE Photon. Technol. Lett. **22**(20), 1473–1475 (2010).
14. H. Choi, S.-W. Cho, J. Kim, and B. Lee, "A thin 3D-2D convertible integral imaging system using a pinhole array on a polarizer," Opt. Express **14**(12), 5183–5190 (2006).
15. A. Saha, K. Bhattacharya, and A. K. Chakraborty, "Reconfigurable achromatic half-wave and quarter-wave retarder in near infrared using crystalline quartz plates," Opt. Eng. **50**(3), 034004 (2011).
16. P. Yeh, "Extended Jones matrix method," J. Opt. Soc. Am. **72**(4), 507–513 (1982).
17. J. Poirson, T. Lanternier, J.-C. Cotteverte, A. L. Floch, and F. Bretenaker, "Jones matrices of a quarter-wave plate for Gaussian beams," Appl. Opt. **34**(30), 6806–6818 (1995).
18. Y. Kim, K. Hong, J. Yeom, J. Hong, and B. Lee, "Optical block module for auto-stereoscopic three-dimensional display," in *Digital Holography and Three-Dimensional Imaging, OSA Technical Digest*, DSu1C (Optical Society of America, 2012).
19. J. Flack, J. Harrold, and G. J. Woodgate, "A prototype 3D mobile phone equipped with a next-generation auto-stereoscopic display," Proc. SPIE **6490**, 1–12 (2007).
20. J. Harrold, D. Wilkes, and G. J. Woodgate, "Switchable 2D/3D display—solid phase liquid crystal microlens array," Proc. IDW **11**, 1495–1496 (2004).

## 1. Introduction

Over the past few years the field of stereoscopic display has developed greatly, including display hardware designs and computational image processing designed to relieve consumers' eye fatigue [1–3]. Two wide-spread methods used in stereoscopic displays use two projectors with polarizing glasses or a high-speed projector (in excess of 120 Hz) with shutter glasses. To avoid a flash from the projector and to increase spacing efficiency, frontal projection-type stereoscopic displays are used in a projection-type stereoscopic display. In such a system, the observer and two projectors are placed side-by-side, as shown in Fig. 1(a).

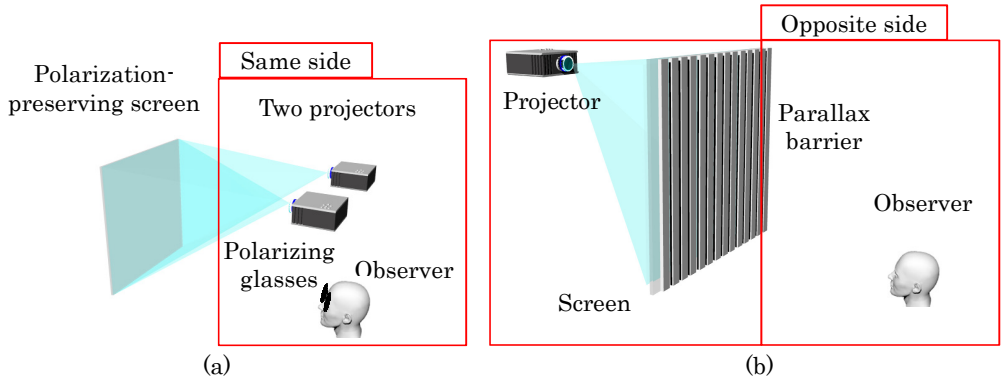


Fig. 1. Two representative projection-type 3D displays: (a) the polarizing glasses method and (b) the parallax barrier method.

Projection-type three-dimensional (3D) displays are vital for a stereoscopic display and an auto-stereoscopic display, such as in the parallax barrier method, the lenticular lens method, and the integral imaging method. They permit spatial and/or temporal multiplexing to produce a larger display and have high-definition because the display devices and the screen are separated [4–6]. One of the major merits of the projection-type auto-stereoscopic display is that only one projector is used. However, such an approach unfortunately limits spacing efficiency because additional optical components, such as a parallax barrier, a lenticular lens, and a lenslet array in front of the screen are needed for delivering different perspectives to the viewer [7,8], even though several methods of reflective projection-type 3D display have been reported [9–12]. This requirement not only makes the projection-type auto-stereoscopic

#168826 - $15.00 USD Received 17 May 2012; revised 24 Jun 2012; accepted 17 Jul 2012; published 20 Aug 2012

display somewhat inconvenient for use in a resource-limited environment, but also partially hinders its applications in the field of projection-type 3D displays, as shown in Fig. 1(b). Therefore, a frontal projection-type auto-stereoscopic display is a rather important step forward as a solution for the success of the 3D display field.

To provide a complementary effort to this important need, we propose here and investigate the frontal projection-type auto-stereoscopic display using a polarizer and a quarter-wave retarding film (QWRF). A schematic diagram of our frontal projection-type auto-stereoscopic display is shown in Fig. 2. In this study, we demonstrate that our proposed display configuration in Fig. 2 can be adapted for two auto-stereoscopic 3D displays, the parallax barrier method, and integral imaging. Because the proposed configuration employs only passive optical components including a polarizer, a QWRF, a polarization-preserving screen, and a parallax barrier or a pinhole array, it could be a useful candidate for use in commercial cinema complexes and might constitute a simple, compact, and cost-effective approach.

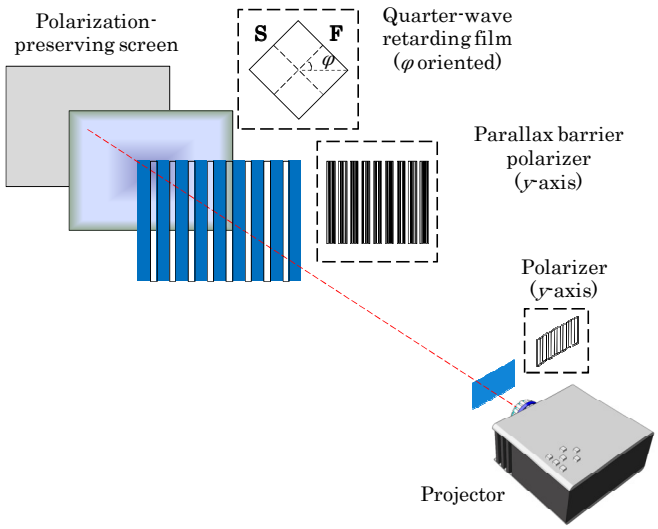


Fig. 2. Concept of the proposed configuration.

## 2. Principle of the proposed scheme

To facilitate physical discussion, let us assume that the horizontal and vertical axes of the polarizer are designated as *x*- and *y*-axes, respectively. Figure 3 shows the light propagation path in the proposed method. Because the polarizer is located in front of the projector, the output light of the projector containing elemental images is polarized along the *y*-axis (*y*-polarized). Because it is *y*-polarized, the *y*-polarized input entering the parallax barrier polarizer emerges from it unchanged. While the output light of the parallax barrier polarizer passes through the QWRF (with its fast axis 45° oriented with respect to the *x*-axis), the light becomes left-circularly polarized. The light is then reflected by the polarization-preserving screen that plays the role of preserving the direction of polarization and reversing the propagation direction of the light. That is to say, the polarization-preserving screen can be regarded as a simple mirror in the description of the state of polarization (SOP). After being reflected from the polarization-preserving screen, therefore, the SOP of the light is converted into being right-circularly polarized. The right-circularly polarized light then meets the QWRF (with its fast axis 135° orientation) again, and the SOP becomes *x*-polarized through the QWRF, resulting in propagation blockage at the *y*-polarized parts of the parallax barrier polarizer.

#168826 - $15.00 USD Received 17 May 2012; revised 24 Jun 2012; accepted 17 Jul 2012; published 20 Aug 2012

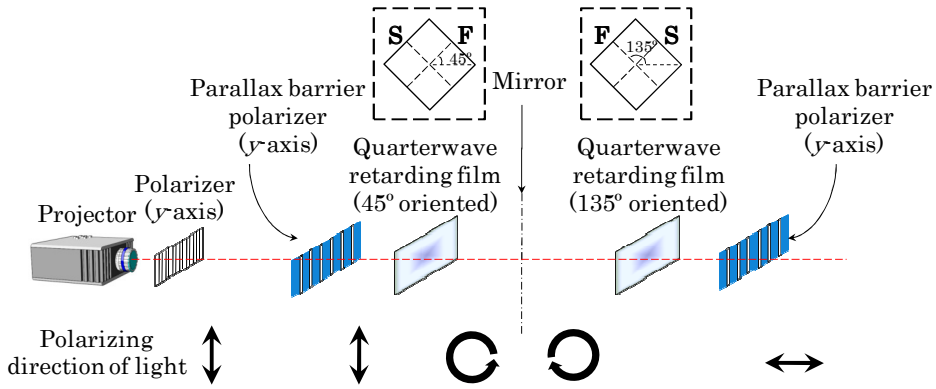


Fig. 3. Path of light propagation in the proposed method.

This physical discussion can be mathematically supported using the Jones formulation [13]. If the optical components are assumed to be ideal ones without any insertion loss, the Jones transfer matrices of the optical components along the light propagation paths in Fig. 3 are expressed as follows:

$$T_{POL} \text{ or } T_{PB} = \begin{bmatrix} 0 & 0 \\ 0 & 1 \end{bmatrix} \left( T_M = \begin{bmatrix} -1 & 0 \\ 0 & 1 \end{bmatrix} \right), \tag{1}$$

$$T_{QWP}(\varphi) = \begin{bmatrix} \cos\varphi & -\sin\varphi \\ \sin\varphi & \cos\varphi \end{bmatrix} \begin{bmatrix} \exp(j\tau/2) & 0 \\ 0 & \exp(-j\tau/2) \end{bmatrix} \begin{bmatrix} \cos\varphi & \sin\varphi \\ -\sin\varphi & \cos\varphi \end{bmatrix}, \tag{2}$$

$$T_S = T_{PB} T_{QWP}(-45°) T_M T_{QWP}(45°) T_{PB} T_{POL}, \tag{3}$$

where $T_{POL}$, $T_{PB}$, $T_{QWP}(\varphi)$, $T_M$, and $T_S$ are the Jones transfer matrices of the front polarizer ($y$-polarized), the polarized part of the parallax barrier ($y$-polarized), the QWRF, the polarization-preserving screen, and the total system except for the projector, respectively. In Eq. (2), $\varphi$ and $\tau$ are the orientation angle and phase retardation ($\pi/2$) of the QWRF, respectively. By means of a simple matrix calculation, it is readily found that $T_S$ becomes a zero matrix. If an elemental image from the projector is represented as an input Jones vector $[A_x, A_y]^t$ where $t$ denotes the transposition of a vector or a matrix, the output Jones vector of the total system becomes $[0, 0]^t$. This implies that any output light component of the projector with an arbitrary SOP cannot transmit the polarized part of the parallax barrier polarizer, and the projector output can only pass through the barrier-free regions of the parallax barrier polarizer. A more detailed principle of the formation of an image is shown in Fig. 4. Although the projected image is not comprised of a pixelated structure, the elemental image is illustrated as a segmented directional image for convenience. The elemental image from the projector can be completely displayed regardless of such polarizing components. In other words, the elemental image can pass through the barrier region and barrier-free region of the parallax barrier polarizer. However, since the elemental image can be observed only through the barrier-free region after reflection on the polarization-preserving screen, the directional view images can be reconstructed by the parallax barrier polarizer with the normal parallax barrier method. Practically, the light intensity at the barrier-free regions of the parallax barrier polarizer is a little brighter than that at the parallax barrier polarizer, which results from the slight insertion loss of the polarizing parts of the parallax barrier polarizer.

#168826 - $15.00 USD Received 17 May 2012; revised 24 Jun 2012; accepted 17 Jul 2012; published 20 Aug 2012

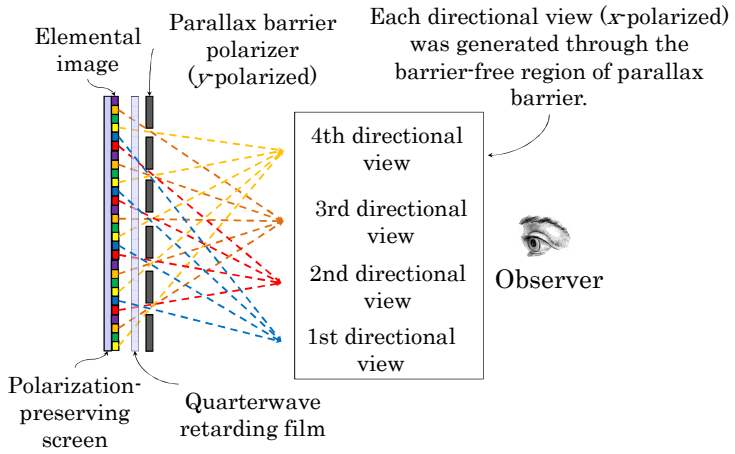


Fig. 4. Principle of image formation of the proposed method in detail.

The polarimetric approach mentioned above can also be applied directly to an integral imaging method if a punctured pinhole array onto a polarizer replaces the parallax barrier polarizer, as shown in Fig. 5. Each ray of the polarization-preserving screen having corresponding information passes through the pinhole array and integrates the 3D image. In this structure, the aperture ratio of the pinhole array determines the differences in optical efficiency. The optical efficiency might be decreased in an integral imaging method when a pinhole array is used as compared with the parallax barrier method [14].

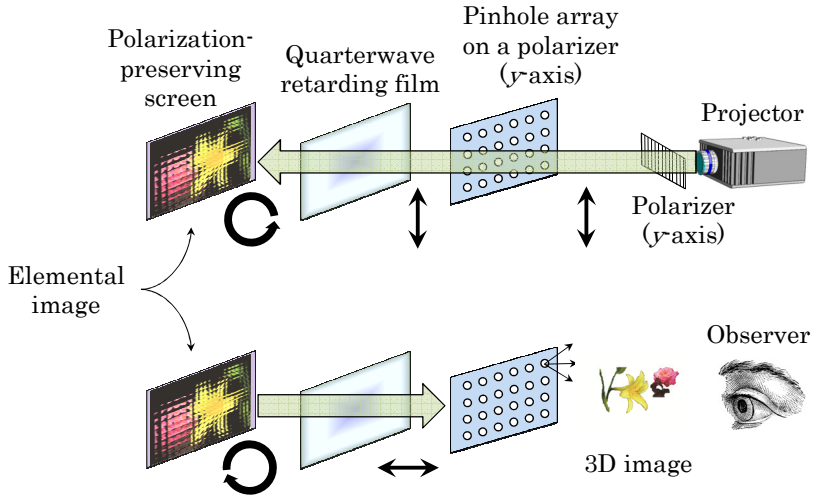


Fig. 5. Application of the proposed method for the integral imaging.

## 3. Crosstalk due to wavelength and incident angle in the proposed method

In QWRFs, phase retardation generally depends on the wavelength and incident angle. Because the QWRF is not optimized over the entire wavelength range of the visible light from the projector, the SOP of the light changes as a function of wavelength when the light meets the QWRF twice. Although a need exists for retarding films that exhibit identical polarization over a broad wavelength range [15], the focus of this study is on analyzing the possibility for crosstalk due to undesirable polarization changes over the visible wavelength range. We used a low-cost, commercially available QWRF (Edmund Optics) in which more than 85% of the light from the projector becomes polarized correctly and the remainder contributes to

#168826 - $15.00 USD Received 17 May 2012; revised 24 Jun 2012; accepted 17 Jul 2012; published 20 Aug 2012

crosstalk due to undesirable transformation of polarization. The other reason for crosstalk is the off-axis illumination of projected light upon the polarization components. As described in Section 2, when the incident light is at a normal angle along the axis of the optical system, perfect transformation of the polarization state can be achieved by passing the light through the optical components, such as a polarizer and a QWRF. However, when the incoming light strikes the optical components at an oblique angle because of off-axis illumination from the projector, leakage that may be responsible for crosstalk can be observed [16,17].

To derive crosstalk due to the wavelength and incident angle of light in the proposed method, let us consider the transmitted wave amplitude of the polarized state. The transmission of light through a polarizer or a QWRF can be given by

$$\begin{aligned}\begin{pmatrix} A_x' \\ A_y' \end{pmatrix} &= \begin{pmatrix} t_x' & 0 \\ 0 & t_y' \end{pmatrix}\begin{pmatrix} \cos\psi & -\sin\psi \\ \sin\psi & \cos\psi \end{pmatrix}\begin{pmatrix} P_{11} & P_{12} \\ P_{21} & P_{22} \end{pmatrix}\begin{pmatrix} \cos\psi & \sin\psi \\ -\sin\psi & \cos\psi \end{pmatrix}\begin{pmatrix} t_x & 0 \\ 0 & t_y \end{pmatrix}\begin{pmatrix} A_x \\ A_y \end{pmatrix} \\ &= T_o R(-\psi) P R(\psi) T_i \begin{pmatrix} A_x \\ A_y \end{pmatrix},\end{aligned} \tag{4}$$

and $t_s$, $t_p$, $t_s'$, and $t_p'$ are the transmission coefficients given by

$$t_x = \frac{2n\cos\theta}{n\cos\theta + n_0\cos\theta_0}, \tag{5}$$

$$t_y = \frac{2n\cos\theta}{n\cos\theta_0 + n_0\cos\theta}, \tag{6}$$

$$t_x' = \frac{2n_0\cos\theta_0}{n_0\cos\theta_0 + n\cos\theta}, \tag{7}$$

$$t_y' = \frac{2n_0\cos\theta_0}{n_0\cos\theta + n\cos\theta_0}, \tag{8}$$

where we recall that $n$ is the index of refraction of air, $n_0$ is the index of refraction of the polarization components, $\theta$ is the incident angle, $\theta_0$ is the refraction angle, $\psi$ is the angle for rotation of coordinate, and $P$ is the matrix representation of polarization components such as a polarizer or a QWRF. $R(-\psi)$ is transformation matrix for the rotation of the coordinate by an angle $\psi$, which can be expressed as

$$\cos\psi = \frac{\cos\theta_0 \sin\phi}{\sqrt{1-\sin^2\theta_0 \sin^2\phi}}, \tag{9}$$

where $\phi$ is the orientation angle of the optic axis of the polarization components [16]. Note that this matrix equation is valid because the polarization components are several micrometers in thickness so that multiple reflections in the components can be neglected. Therefore, when we set the number of views of the system, the position of the observer and polarization components, and the matrix representation of polarization components ($\psi_{QWP} = \pi/4$ and $\psi_{POL} = \pi/2$, respectively), the transmissions of the light can be written explicitly as

$$\begin{pmatrix} A_x' \\ A_y' \end{pmatrix} = T_o R(-\psi_{QWP}) P_{QWP} R(\psi_{QWP}) T_i \begin{pmatrix} A_x \\ A_y \end{pmatrix}, \tag{10}$$

#168826 - $15.00 USD Received 17 May 2012; revised 24 Jun 2012; accepted 17 Jul 2012; published 20 Aug 2012

$$\begin{pmatrix} A_x' \\ A_y' \end{pmatrix} = T_o R(-\psi_{POL}) P_{POL} R(\psi_{POL}) T_i \begin{pmatrix} A_x \\ A_y \end{pmatrix}. \tag{11}$$

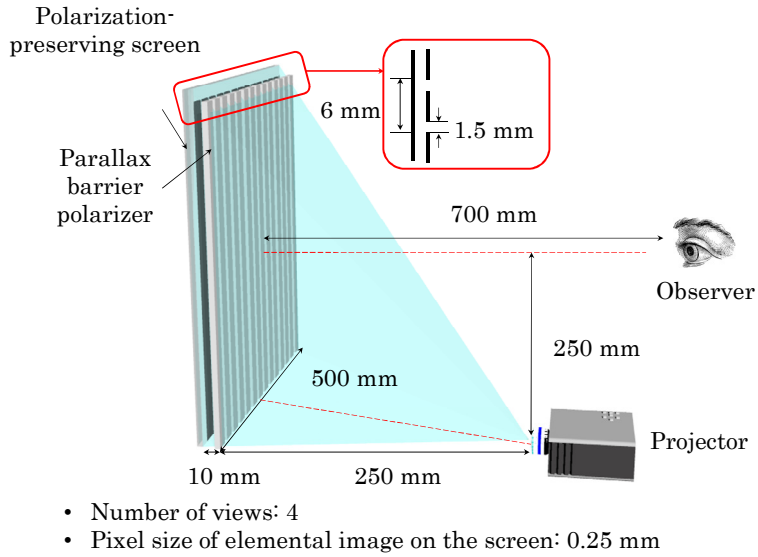


Fig. 6. Simulation configuration for verifying the proposed method.

As an example, we analyzed the transmission ratio of the incident light in the case of the parallax barrier method. Figure 6 provides information on the simulation conditions of the frontal projection-type auto-stereoscopic display. The observer was located at a distance of 700 mm in front of the parallax barrier. The size of the slit was 1.5 mm and the space between the slits was 6 mm so that the system could have 4 views. The projector was located at a distance of 250 mm below the observer, and the projected light was polarized into *y*-polarization. The QWRF was optimized at a wavelength of 560 nm and the phase retardation ratio was supposed to increase or decrease linearly. The retardation ratio is 0.25 at a wavelength of 560 nm, according to data provided by Edmund Optics, and the maximum and minimum values of the retardation ratio are 0.30 and 0.20, respectively. We assumed that the elemental image from the projector had a Lambertian emission profile and that it was composed of 1024 × 1024 pixels. Also, we assumed that the polarization-preserving screen acts as a simple mirror in the simulation. Since the elemental images on the polarization-preserving screen are incident obliquely after passing through the parallax barrier polarizer and a QWRF, the transmission ratio of the elemental image could decrease at the plane of the screen. In the same manner, rays travelling through the screen and polarizer arrived at the observer's eye at an oblique angle. This entailed undesirable crosstalk horizontally as well as vertically. Figure 7 shows the transmission ratio on the observation plane along the horizontal direction from −750 mm to 750 mm, in which the transmission ratio is defined as the normalized value of $\sqrt{|A_x'|^2+|A_y'|^2}$. The red dotted line indicates the transmission ratio for the ideal case using a normal parallax barrier. The blue line indicates the transmission ratio of the proposed method. Since the parallax barrier was made by polarizer and a QWRF was located in front of it, the transmission ratio decreased. When we adopted a QWRF and a parallax barrier polarizer, it was found that the transmission ratio was 5% different in the normal direction and 8% different on the edge of the observation plane as compared with the conventional parallax barrier.

#168826 - $15.00 USD Received 17 May 2012; revised 24 Jun 2012; accepted 17 Jul 2012; published 20 Aug 2012

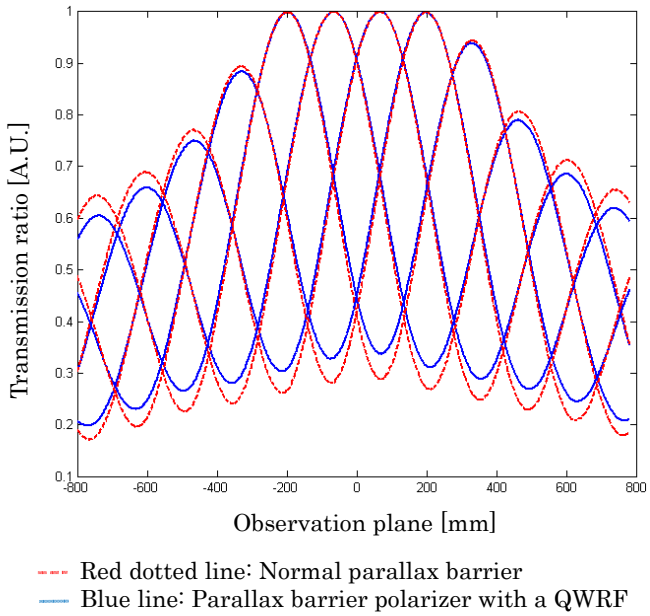


Fig. 7. Transmission ratio on the observation plane along the horizontal direction. The transmission ratio was observed at the observation plane along the lateral direction.

## 4. Experimental results

To demonstrate the theoretical prediction, several preliminary experiments were performed using a polarizer and a QWRF. A high-definition projector (Panasonic PT-AE100E) with a resolution of 1920(H) × 1080(V) was used as the display device. To avoid direct reflection of the projected light on the surface of the polarizer, an anti-reflection-coated polarizer was employed as a parallax barrier or pinhole array [18].

The parallax barrier and pinhole array were fabricated using a laser-punctuated machine. Each parallax barrier had a size of 1.5 mm and the space between slits was 6 mm. The pinhole array was composed of 34(H) × 24(V) apertures, each with a size of 2 mm. The space between apertures was set to 10 mm and therefore the aperture ratio of the pinhole array was about 3.1%. A QWRF (Edmund Optics) was used to change the state of the polarized light. The boundaries of the QWRF and the polarizer were attached by an acrylic plate, and the acrylic plate permitted the distance between them and the polarization-preserving screen to be maintained at 10 mm. Two images, 'blue car' and 'red car', were used in the parallax barrier experiment, and two character images, 'S' and 'U', were used in the integral imaging experiment. The image of the 'blue car' was formed at 200 mm in front of the parallax barrier, and the image of the 'red car' appeared 200 mm behind the parallax barrier. The images of two letters 'S' and 'U' were formed 50 mm in front of and behind the pinhole array, respectively.

Figure 8 shows the experimental results observed from different perspectives for both the parallax barrier method and integral imaging. In spite of the fact that the polarizing components were located in front of the screen, the elemental image was successfully generated. The captured images shown in Fig. 8(a) were left- and right-end-view images for the parallax barrier method, and the photos in Fig. 8(b) were captured from the horizontal and vertical positions. Each directional-view image was well-separated at corresponding positions, as shown in Fig. 8. These findings, therefore, verify the frontal projection method of the proposed method.

#168826 - $15.00 USD Received 17 May 2012; revised 24 Jun 2012; accepted 17 Jul 2012; published 20 Aug 2012

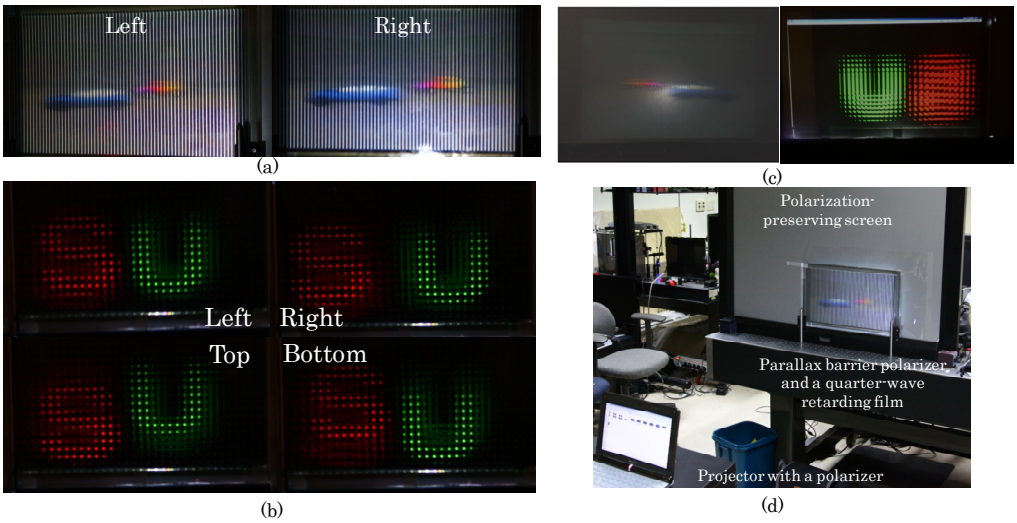


Fig. 8. Experimental results for (a) the parallax barrier polarizer, (b) integral imaging by using pinhole array method, (c) photo of the elemental image captured behind the screen, and (d) experimental setup of the proposed method.

## 5. Conclusions

In this paper, we introduced a novel frontal projection-type auto-stereoscopic display method using a single projector with passive optical elements, such as a polarizer and a QWRF. This compact and cost-effective frontal projection-type auto-stereoscopic display technique, which is based on the parallax barrier method or integral imaging, requires neither complicated structures nor any active optical/mechanical components, so it is facile and inexpensive. The principle of the proposed method was verified experimentally for both the parallax barrier method and integral imaging using a pinhole array method, thus confirming its feasibility. We believe that the proposed method will be useful for glasses-free projection-type 3D displays because of the saving of space as well as cost for the next step of 3D theaters. Finally, further research directed toward passive polarization-activated lens arrays will be required for frontal projection-type auto-stereoscopic displays based on the lenticular lens method [19,20].

## Acknowledgment

This research was supported by the Brain Korea 21 Program (Information Technology, Seoul National University).

#168826 - $15.00 USD Received 17 May 2012; revised 24 Jun 2012; accepted 17 Jul 2012; published 20 Aug 2012